

Recycling of Ethylene Propylene Diene Monomer (EPDM) Waste. III. Processability of EPDM Rubber Compound Containing Ground EPDM Vulcanizates

Ceni Jacob, A. K. Bhattacharya, A. K. Bhowmick, P. P. De, S. K. De

Rubber Technology Centre, Indian Institute of Technology, Kharagpur 721 302, West Bengal, India

Received 10 December 2001; accepted 7 May 2002

ABSTRACT: The rheological behavior of ethylene propylene diene monomer (EPDM) compounds containing ground EPDM waste (W-EPDM) of known composition was studied by using a Monsanto processability tester in a temperature range of 90–110°C and a shear rate range of 306.7–1533.24 s⁻¹. It is found that the shear viscosity decreases slightly with increasing W-EPDM loading because of wall slip that results from the migration of lubricants from the W-EPDM. The addition of W-EPDM to raw EPDM results in

a decreased die swell at all temperatures and shear rates. SEM photomicrographs of the EPDM extrudate surface show improved surface smoothness and reduced extrudate distortion when EPDM is blended with W-EPDM. © 2003 Wiley Periodicals, Inc. *J Appl Polym Sci* 87: 2204–2215, 2003

Key words: ethylene propylene diene monomer; waste recycling; ground vulcanizate; processability; die swell

INTRODUCTION

Waste rubbers, particularly worn-out automobile tires, constitute a major proportion of nonbiodegradable wastes. The disposal problems created by waste rubber vulcanizates can be effectively minimized by reutilization of their ground form. There are reports on the utilization of rubber compounds containing ground rubber tires that are obtained by the cryogenic or ambient grinding of the worn-out tires.^{1–6} The utility of a rubber compound is determined by its processing characteristics, vulcanizate properties, and cost. Because polymeric compounds are non-Newtonian in their flow behavior, a study of their flow characteristics as a function of shear rate, compound formulation, and temperature of extrusion is important in order to optimize the processing conditions. The processability of a rubber compound depends not only on the polymer type, average molecular weight, molecular weight distribution, and temperature but also on the type and concentration of filler, polymer–filler interaction, processing aids, and scorchiness of the compound.^{7,8} Phadke⁹ observed that the addition of cryoground rubber causes a reduction in the melt viscosity of a natural rubber compound, and Gibala et al.¹⁰ observed an increase in the Mooney viscosity of a styrene butadiene rubber compound upon the incor-

poration of ground rubber. Dimensional instability and extrudate distortion are the two major problems of rubber extrusion.¹¹ It has been reported that the addition of crosslinked particles to a fresh rubber compound results in decreased die swell, a smoother surface finish, and better shape retention.¹²

Ethylene propylene diene monomer (EPDM) rubber is unique in the sense that it can be extended by high loadings of oil and filler. Earlier workers studied the rheological properties of EPDM neat rubber¹³ and EPDM compounds filled with carbon black and oil.^{14–16} Both the neat rubber and filled compounds show pseudoplasticity. Bhaumuik et al.¹⁷ reported the rheological behavior of blends of EPDM and brominated butyl rubber.

The weather resistance of EPDM rubber is excellent, so it is useful in many outdoor applications. However, there has been no systematic investigation on the utilization of EPDM rubber waste (W-EPDM). Jacob et al. reported that ground vulcanizate of a known composition (W-EPDM) shows the characteristics of reinforcing fillers, possibly by virtue of the high carbon black content, when incorporated into gum (unfilled) EPDM matrix (raw EPDM or R-EPDM).¹⁸ They also reported that W-EPDM can replace 45% of the EPDM in a thermoplastic elastomeric EPDM/polypropylene blend.¹⁹ The present article, the third in the series, reports the results of our studies on the processability of the EPDM compounds filled with W-EPDM using a Monsanto processability tester in the normal range of shear rates and temperatures used in processing rubber compounds.

Correspondence to: S. K. De (skde@rtc.iitkgp.ernet.in).

Contract grant sponsor: Ministry of Environment and Forests, Government of India, New Delhi.

TABLE I
Physical Properties of Aged EPDM Vulcanizate Used for Preparation of Ground Rubber (W-EPDM)

Tensile Strength (MPa)	Elongation at Break, (%)	Modulus at 100% Elongation (MPa)	Tear Strength (KN/m)	Tension Set (100% Elongation) (%)	Shore A Hardness
7.01 (7.04)	260 (430)	3.31 (2.18)	31.5 (33.0)	4 (4)	64 (55)

Formulation (phr by weight): EPDM, 100; GPF, carbon black, 120; Sunpar 2280 oil, 70; poly(ethylene glycol), 1.5; paraffin wax, 10; brown factice, 10; zinc oxide, 5; 2,2,4-trimethyl 1,2 dihydroquinoline (Accinox TQ), 0.5; stearic acid, 1.0; sulfur, 1.5; zinc dimethyldithiocarbamate, 2.0; tetramethyl thiuramdisulfide, 1.2; and mercaptobenzothiazole, 1.2; cure for 14 min at 150°C. The values in parentheses are for the aged samples.

EXPERIMENTAL

Materials

The EPDM rubber used in the study was Royalene 521 (Uniroyal Chemical Company). It has an ethylene/propylene ratio of 52/48 and an ethylidene norbornene content of 4.9%. Other ingredients were rubber grade chemicals obtained locally.

Preparation of ground EPDM vulcanizate

The ground rubber was prepared from EPDM vulcanizate of known composition (Table I). The physical properties of the EPDM vulcanizate before and after aging (Table I) were determined according to ASTM standards. Thick (~10 mm) vulcanizate samples were prepared by an additional 5 min molding over and above the optimum cure time of 14 min at 150°C. The vulcanizate was aged at 100°C for 48 h in order to simulate the long storage conditions of factory scraps or the service life of postconsumer waste. The aged EPDM vulcanizate was mechanically ground to the powder form using a mechanical grinder (Ralliwolf TG-6 Bench Grinder) with a silicon carbide abrasive wheel rotating at 2950 rpm. The ground EPDM vulcanizate is designated as W-EPDM.

The gum W-EPDM ground rubber [W-EPDM(G)] was prepared by following the same procedure. The formulation used here was similar to that in Table I but without carbon black and plasticizers.

SEM Studies of W-EPDM

As obtained, the W-EPDM exists in a highly aggregated form.^{18,20} It was ultrasonically dispersed using the following method. The powder was poured into a beaker containing about 50 mL of water at room temperature, and the beaker was placed in an ultrasonic bath (Imeco Ultrasonics, Mumbai, India), which is a stainless steel tank (350 × 300 × 250 mm) connected to a transistorized ultrasonic generator. Mechanical energy in the form of high intensity, high frequency sound waves (frequency 20 ± 3 kHz) was introduced into the water in the bath, which separated the particles in the beaker. A mount was immersed into the

beaker to collect the dispersed particles. The separated particles were dried, gold coated, and examined under a Cam Scan Series 2 scanning electron microscope (Cambridge Scanning Co. Ltd.) in order to study the particle size and surface characteristics.

Before being subjected to ultrasonic treatment, the W-EPDM was also examined under SEM.

Mixing

The formulations are given in Table II. Mixing was done on a two-roll mill (6 × 13 in., Schwabenthan) as per the standard procedure (ASTM D 3182).

Processability studies

Rheological studies were carried out using a Monsanto processability tester (MPT, model 83077). The capillary that was used had a length/depth (L/D) ratio of 30:1 and multiple entry angles of 45° and 60°. The test program selected for the study had four extrusion zones corresponding to shear rates of 306.7, 613.2, 1226.4, and 1533.24 s⁻¹ and a die swell pause of 30 s.

About 10–12 g of the rubber compound, depending upon its density, was placed in the heated barrel of the MPT.^{11,12} After a preheating time of 3 min, the compound was forced through the capillary at the other end of the barrel by the downward movement of the

TABLE II
Formulations Containing W-EPDM

Ingredients	Mix Number					
	W ₀	W ₂₀	W ₄₀	W ₅₀	W ₆₀	W ₁₀₀
R-EPDM	100	100	100	100	100	100
W-EPDM	0	20	40	50	60	100
ZnO	5.0	5.0	5.0	5.0	5.0	5.0
Stearic acid	1.0	1.0	1.0	1.0	1.0	1.0
TMTD	1.0	1.0	1.0	1.0	1.0	1.0
MBT	0.5	0.5	0.5	0.5	0.5	0.5
Sulfur	1.5	1.5	1.5	1.5	1.5	1.5

R-EPDM, raw EPDM; W-EPDM, waste EPDM (laboratory made); ZnO stearic acid, activators; TMTD, tetramethylthiuram disulfide; MBT, mercaptobenzothiazole.

piston, which was heated to the same temperature, at a constant rate corresponding to the selected shear rate in that zone. The extrusion pressure was recorded by a transducer mounted in the barrel just above the entry to the die.

The apparent wall shear rate ($\dot{\gamma}_{app}$), apparent wall shear stress (τ_{app}), and apparent viscosity (η_{app}) at 90, 100, and 110°C were calculated according to the following equations²¹:

$$\tau_{app} = \frac{\Delta P}{4(L/D)} \quad (1)$$

$$\dot{\gamma}_{app} = \frac{32r_B^2 v}{D^3} \quad (2)$$

$$\eta_{app} = \frac{\tau_{app}}{\dot{\gamma}_{app}} \quad (3)$$

where ΔP is the pressure drop across the length of the capillary, r_B is the barrel radius, v is the piston rate, and D and L are the diameter and length of the capillary, respectively.

Correction to data

The apparent shear rate was converted to the true shear rate by applying Rabinowitch correction^{21,22}:

$$\dot{\gamma}_w = \frac{(3n' + 1)}{4n'} \dot{\gamma}_{app} \quad (4)$$

where n' is the slope of the line obtained by plotting $\log \dot{\gamma}_{app}$ against $\log \tau_{app}$.

It was found that at sufficiently large L/D and the multiple angles used here, the entry effect of the die and the pressure drop were minimized. Representative Bagley plots for the gum compound (W_0) and a filled compound (W_{100}) at 110°C and 1533.2 s⁻¹ are given in Figure 1. The correction factor for the L/D was found to be less than 2.5 for the compounds, leading to negligible changes in the apparent shear stress at the high L/D ratio (30/1) used in the present study. Therefore, the apparent shear stress can be taken as the true shear stress for the compounds studied here (Table II). Accordingly, the calculated shear viscosity may be assumed to be the true shear viscosity of these compounds.

Die swell and extrudate distortion

The extrudate diameter was measured by a die swell detector with a scanning He-Ne laser beam. The percentage of die swell is given as

$$\% \text{ die swell} = \frac{D_e - D_c}{D_c} \times 100 \quad (5)$$

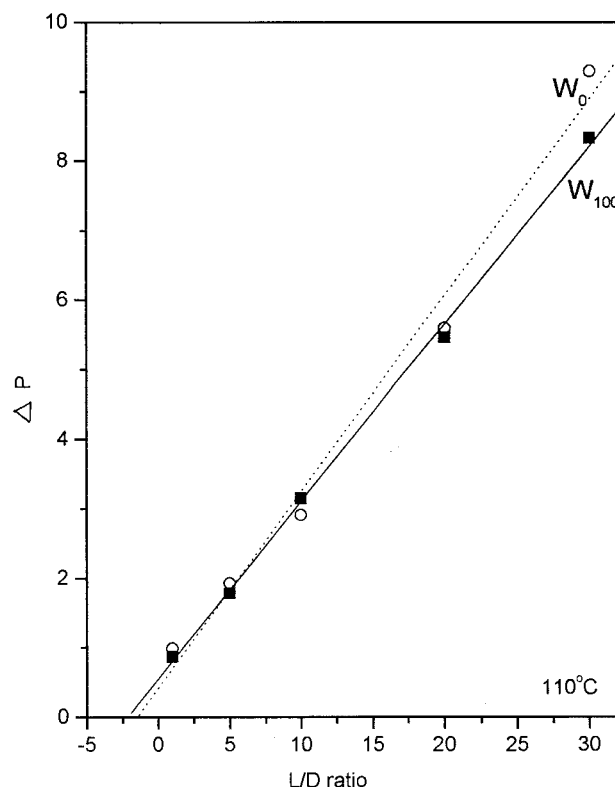


Figure 1 Representative plots of the barrel pressure against the L/D ratios of the capillaries for W_0 and W_{100} compositions (Bagley correction).

where D_e and D_c are the diameters of the extrudate and capillary, respectively. The swelling ratio (α) is given by D_e/D_c . The extrudates coming out through the die at different shear zones were collected separately and the surface irregularities were studied using a scanning electron microscope (JSM 5800, Jeol) after gold coating of the samples.

Stress relaxation

The stress relaxation times of the compounds were determined by moving the piston quickly after the fourth zone before the end of the piston run and then stopping suddenly. The barrel pressure just at the time of the stopping of the piston and the time required to relax 90% of this stress were recorded automatically. The stress relaxing behavior of the compounds was studied from the plots of the barrel pressure versus the time of relaxation.

Elastic energy of compounds

A portion of the energy supplied to the rubber compound in the shear flow is converted into heat (viscous

TABLE III
Formulations of Control Compounds for Studying Role of Filler, Oil, and Crosslinked Gum EPDM [W-EPDM (G)] on the Processability of EPDM

Ingredients	Mix No.					
	W_0	W_{20}	W_{20G}	W_{20B}	W_{20L}	W_{20GBL}
R-EPDM	100	100	100	100	100	100
W-EPDM	—	20	—	—	—	—
W-EPDM(G)	—	—	7.0	—	—	7.0
Carbon black	—	—	—	7.4	—	7.4
Oil	—	—	—	—	4.3	4.3
ZnO	5	5	5	5	5	5
Stearic acid	1.0	1.0	1.0	1.0	1.0	1.0
TMTD	1.0	1.0	1.0	1.0	1.0	1.0
MBT	0.5	0.5	0.5	0.5	0.5	0.5
Sulfur	1.5	1.5	1.5	1.5	1.5	1.5

energy dissipation) and the remaining part is stored in the form of elastic energy, which is recoverable at the die exit.^{12,23,24} It is well known that the die swell and stress relaxation characteristics of the rubber compound depend upon the stored elastic energy in the compound.

The elastic energy stored per unit volume (E_e) of the compound is given as²⁴

$$E_e = \tau \gamma_m C \quad (6)$$

where γ_m is the maximum recoverable deformation. The value of γ_m was calculated according to the following equation²⁴:

$$\gamma_m \sqrt{(1/2C)(\alpha^{-4} + 2\alpha^2 - 3)} \quad (7)$$

where α is the swelling index and $C = (3n' + 1)/4(n' + 1)$, where n' is determined from the slope of the line obtained by plotting $\log \tau_{app}$ against $\log \dot{\gamma}_{app}$ and $n' = n$ when n' remains constant for the range of shear rates studied.

Critical shear rate

Because the compounds exhibited distortion in the range of shear rates used for the study, the rheological behavior of representative compounds at lower shear rates (10 – 250 s^{-1}) was also studied. The shear rate beyond which melt fracture occurred was taken as the critical shear rate ($\dot{\gamma}_{crit}$).²²

Effect of individual ingredients present in crosslinked particles (W-EPDM) on rheological behavior of rubber compounds

It is known that the rheological behavior of rubber compounds is modified by the presence of fillers and plasticizers. The influence of individual ingredients like carbon black, oil, and crosslinked rubber, which are present in the W-EPDM, on the rheological behav-

ior of EPDM compounds was studied using compounds containing carbon black, oil, and crosslinked rubber (gum) particles in the shear rate range of 306 – 1533 s^{-1} at different temperatures. The formulations used for the study are given in Table III. The formulations contain carbon black, oil, and crosslinked rubber (gum particles) in amounts equivalent to that present in 20 phr of W-EPDM. The compounds were prepared on a two-roll mill as per the standard procedure at constant nip gap.

RESULTS AND DISCUSSION

Properties of EPDM vulcanizate used for making ground W-EPDM

The physical properties of the vulcanizate used for making the powder are given in Table I. Aging of the vulcanizates results in the formation of a tighter network, as can be seen by the increased modulus and hardness and decreased elongation at break.

W-EPDM particle characteristics

The SEM photomicrographs of W-EPDM are given in Figure 2. The spongy and branched chainlike aggregates shown in Figure 2(a) are broken down into smaller aggregates and individual particles [Fig. 2(b)] by the ultrasonic dispersion technique. A typical particle ($\sim 30 \mu\text{m}$) is shown in Figure 2(c). The particle sizes vary from 5 to $60 \mu\text{m}$. The particle size distribution is shown in Figure 3. The surface of the particles is found to be rough and convoluted.

Pseudoplasticity of compounds

The log–log plots of τ_{app} and $\dot{\gamma}_{app}$ for the compounds at 90 , 100 , and 110°C are given in Figure 4. It is evident that all compounds are pseudoplastic, but the gum compound (without W-EPDM) does not obey the Power law at any temperature. Compounds contain-

ing low amounts of W-EPDM follow the Power law at 90°C but not at 100 and 110°C. However, the compounds filled with high amounts of W-EPDM follow the Power law equation²² at all temperatures:

$$\tau_{\text{app}} = k(\dot{\gamma}_{\text{app}})^n \quad (8)$$

where n is the power law index, which is a measure of the pseudoplasticity of the compound, and k is the consistency index. The n values vary from 0.05 to 0.08 for the different rubber compounds.

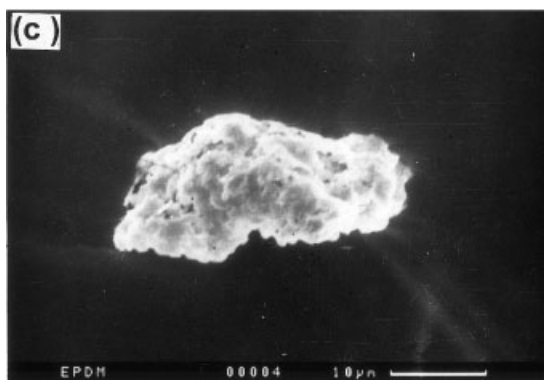
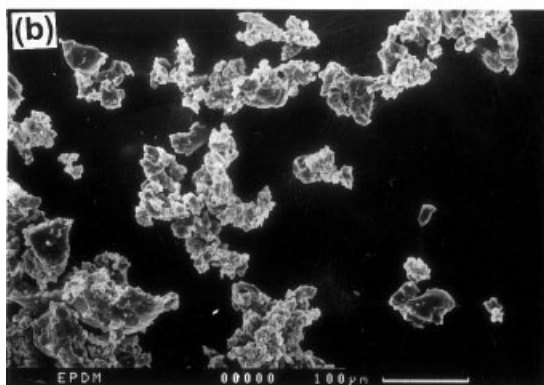


Figure 2 SEM photomicrographs of the powdered vulcanizate (W-EPDM) (a) chainlike aggregates, (b) low structured aggregates and particles after ultrasonic dispersion, and (c) a single particle at higher magnification.

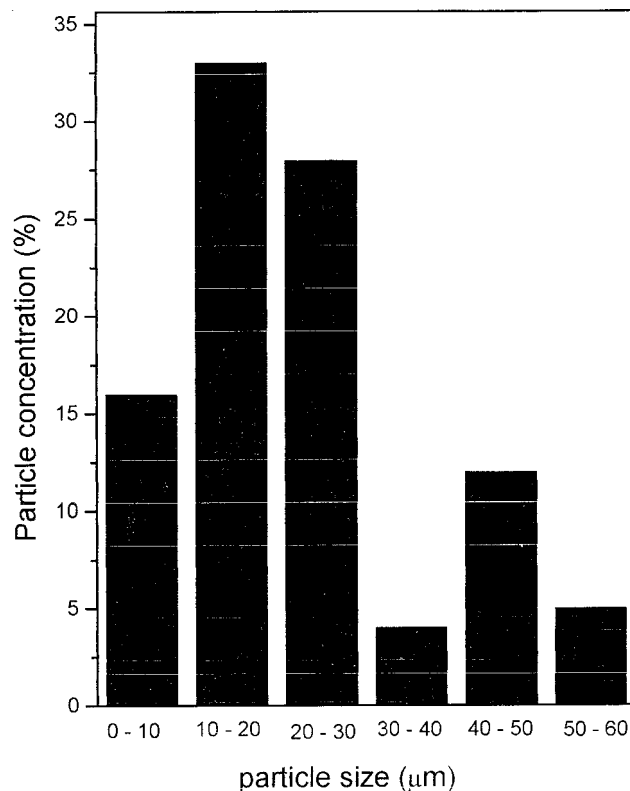


Figure 3 The particle size distribution of W-EPDM.

Shear viscosity: Effect of W-EPDM loading, shear rate, and temperature

The plots of the shear viscosity versus the W-EPDM content at different apparent shear rates and temperatures are given in Figure 5. At all shear rates at 110°C and at higher shear rates at 100°C the addition of W-EPDM results in a reduction of viscosity. At all shear rates at 90°C and at lower shear rates at 100°C the viscosity first decreases with 20 phr W-EPDM and then increases with the progressive addition of W-EPDM. As Roy et al.²⁵ reported, two opposing factors might contribute to the viscosity of the filled compound. First, the viscosity increases upon the addition of W-EPDM because of a rubber–filler interaction, which comes from the carbon black filler present in W-EPDM; second, the viscosity decreases because of wall slip, which is found to increase with the rate of shear and temperature. In the present case the decrease in viscosity is the result of wall slip contributed by the migration of oil from W-EPDM. Wall slip is enhanced by the presence of a thin lubricating layer between the rubber compound and the capillary wall.^{26–28} This may result in lower shear stress values when compared to the no-slip condition. Studies have shown that lubricants and plasticizers can migrate from the powdered rubber phase to the base rubber matrix.^{29–31} Such plasticizer migration is likely to occur in the EPDM compound containing W-EPDM,

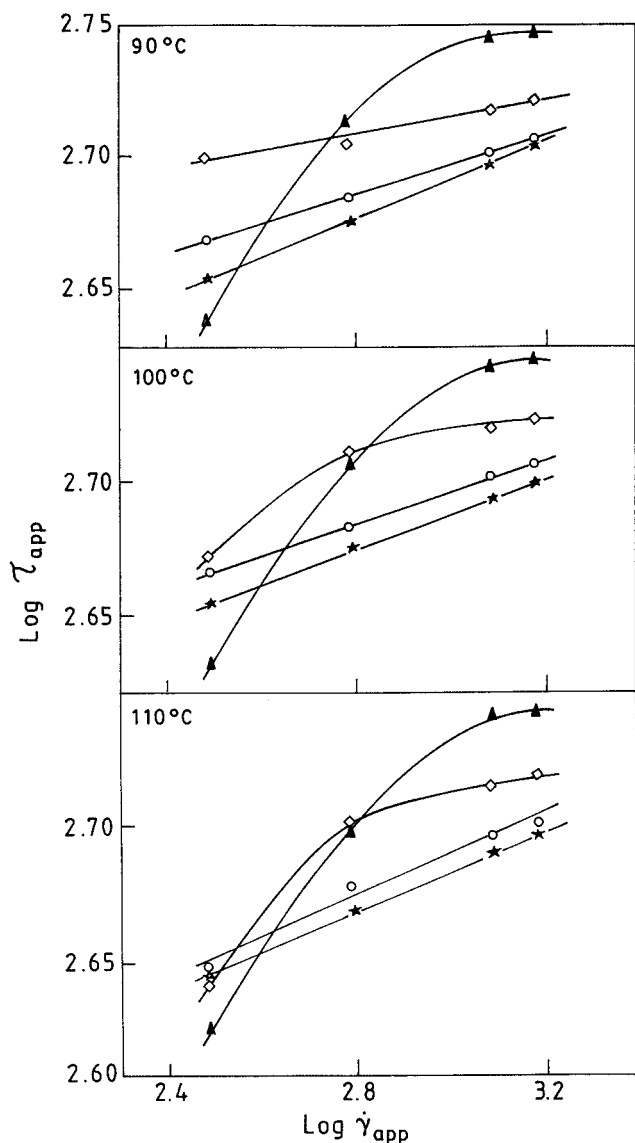


Figure 4 Log-log plots of the shear stress (τ_{app}) and shear rate ($\dot{\gamma}_{app}$) at (a) 90, (b) 100, and (c) 110°C (τ_{app} in kPa and $\dot{\gamma}_{app}$ in s^{-1}) for representative compositions: (\blacktriangle) W_0 , (\diamond) W_{20} , (\circ) W_{60} , and ($*$) W_{100} .

which is highly oil extended (70 phr). The plasticizer migration increases the slip, especially at higher shear rates and temperatures. This has been confirmed by studies at lower shear rates, as discussed later. At 90°C, as the loading of W-EPDM increases, the rubber-filler interaction overshadows the slip, resulting in a slight increase of the viscosity, whereas an increase of temperature further enhances the wall slip, leading to a drop in viscosity at 100 and 110°C.

At constant loading of W-EPDM, the effect of the temperature on the shear viscosity is negligible for the highly loaded compounds, as well as the gum compound, whereas for the lightly loaded compounds the viscosity increases with the increase in temperature [Fig. 5(b)]. Isayev and Wan³² reported that in the

presence of curatives the viscosity of rubber compounds depends not only on the temperature and shear rate but also on the state of cure. As the temperature increases the viscosity decreases because of the increased kinetic energy of the molecules, but it is counterbalanced by the onset of vulcanization at higher temperatures. Hence, the unexpected increase of viscosity with temperature may be attributed to the onset of curing in the compounds. As reported in an earlier article,¹⁸ the Mooney scorch time at 120°C for the compounds is drastically reduced by the addition of W-EPDM (33 min for W_0 to 18 min for W_{20}) and thus W_0 is less likely to be cured as compared to the W-EPDM filled compounds. As the W-EPDM loading increases, the volume fraction of virgin EPDM decreases. Therefore, the effect of crosslinking progressively decreases, resulting in a negligible change of viscosity for the highly loaded compound (W_{100}) with increasing temperatures.

Stress relaxation

The stress relaxation time is determined by the elastic energy stored in the compound, as well as the compound viscosity. As the viscosity of the compound decreases, the relaxation of the stress will be faster even if the stored elastic energy is greater. Moreover, in a multicomponent compound where the rubber as well as the filler (the crosslinked polymer in W-EPDM) are deformable and able to relax the stress, the relaxation times of both R-EPDM and W-EPDM contribute to the overall relaxation of the system. As seen in Table IV, the initial stress (Γ_i) decreases with the W-EPDM loading, indicating the decreasing amount of energy stored in the compounds. But as the viscosity of the compounds under low shear rate conditions drastically increases with W-EPDM loading,¹⁸ the relative ease with which the stress relaxes in a constant strain diminishes, hence the longer relaxation time (t_c). Furthermore, the stress relaxation of the crosslinked particles is slower than the R-EPDM chains, which in turn can result in increased relaxation time with an increasing amount of W-EPDM. This is found to be true at the three temperatures studied. Figure 6 shows the stress relaxation behavior of the representative compositions at 110°C.

Table IV also shows the effect of temperature on the stress relaxation time (for 60% decay of the initial stress) of the compounds. As the temperature rises, the mobility of the polymer chains increases, which may result in a faster relaxation process.

Extrudate distortion

Incorporation of W-EPDM decreases the severity of distortion (i.e., screw-thread appearance) of the extrudate, implying that the addition of W-EPDM lowers the proportion of elastic strain of the compound in the

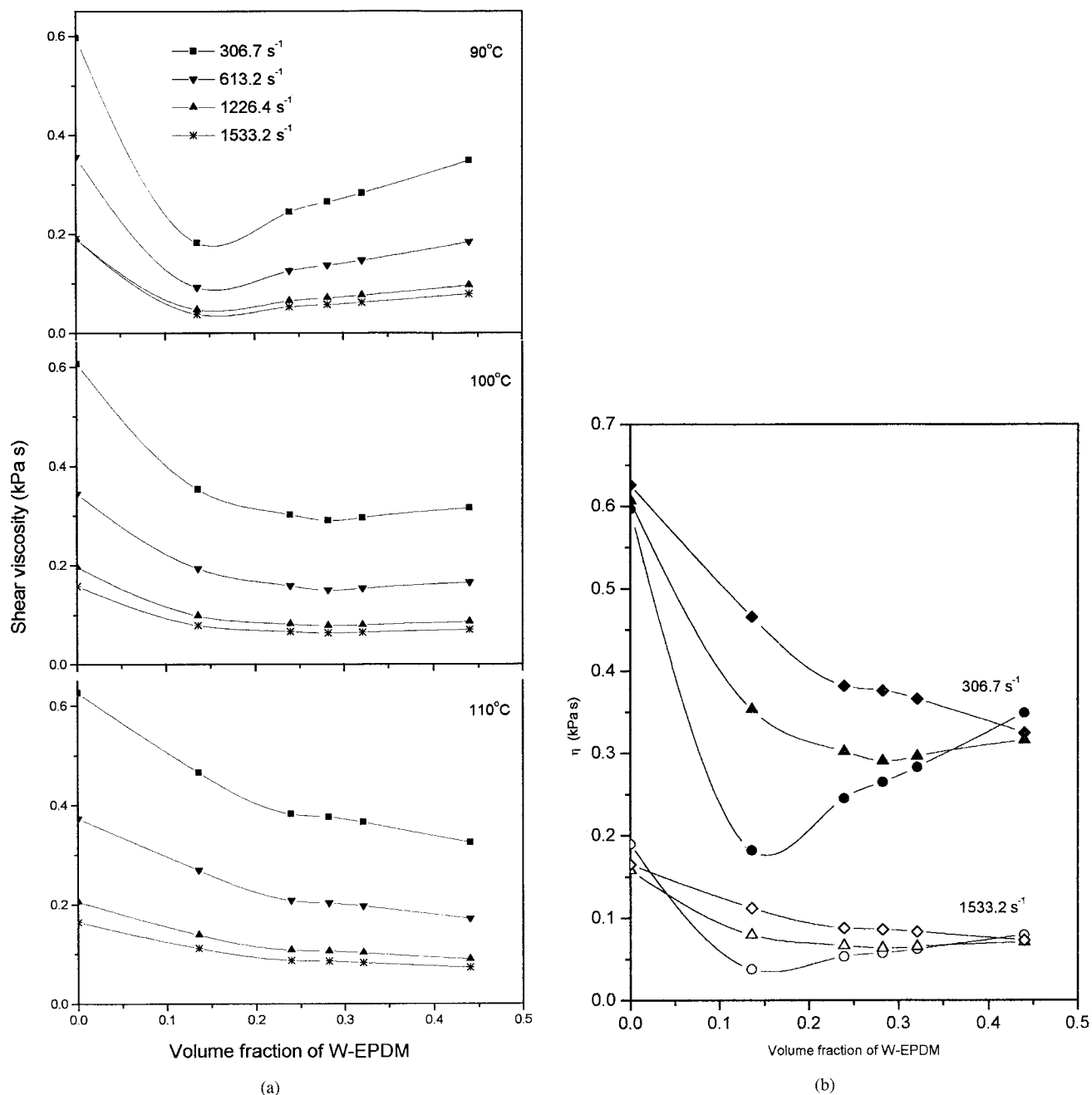


Figure 5 The variation of the shear viscosity (η) with the W-EPDM content with the (a) effect of shear rate and (b) effect of temperature at (○, ●) 90, (▲, △) 100, and (◇, ◆) 110°C.

stress field.³³ Figure 7(a–c) displays SEM photomicrographs of the representative extrudates at 110°C. The higher viscosity of the filled compound in the low stress region outside the die may also provide an increased resistance to the distortion.

Die swell

The addition of W-EPDM reduces the die swell at all shear rates and temperatures as shown in Figure 8. Rosen and Rodriguez¹² reported that the presence of

TABLE IV
Results of Stress Relaxation Studies

Mix No.	Initial Stress (kPa)			Time for 60% Relaxation (s)		
	90°C	100°C	110°C	90°C	100°C	110°C
W_0	549.9	555.1	554.5	6.6	5.1	6.0
W_{20}	528.1	527.5	525.2	12.6	8.4	8.0
W_{40}	514.8	512.5	509.7	14.4	10.2	8.4
W_{50}	513.7	510.2	508.0	16.8	12.0	12.6
W_{60}	510.3	506.8	503.9	18.6	12.6	10.8
W_{100}	506.2	498.2	497.6	21.0	18.6	17.4

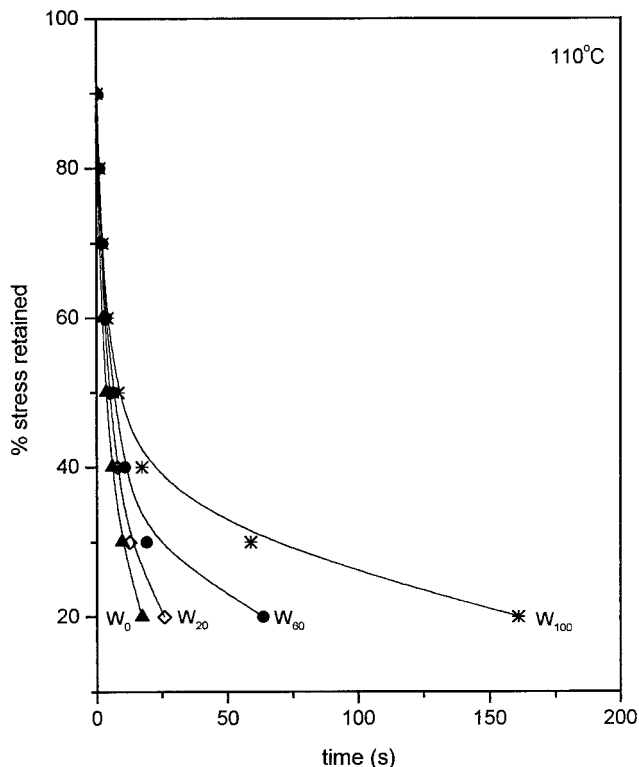


Figure 6 The stress relaxation behavior of the representative compounds at 110°C.

gel reduces the amount of energy that can be elastically stored by the material. The more tightly crosslinked the particle is, the smaller the amount of energy it can absorb by itself, thereby reducing the total energy storing capacity of the system. Hence, the elastic recovery outside the stress field will be less when the crosslinked rubber particles are present, resulting in lower die swell of the extrudate. The high melt fracture shown by the gum compound may also be the reason for the apparent high die swell of the gum, as well as the compounds containing lower amounts of W-EPDM. Figure 9 shows the dependence of the elastic energy on W-EPDM loading and shear rate. At all shear rates and temperatures, an increase in the W-EPDM content causes the elastic energy to decrease, which is in agreement with the observation of decreasing die swell with the progressive addition of W-EPDM.

It is also observed that with an increasing shear rate the die swell decreases, especially for the gum and lightly filled compounds whose extrudates show high melt fracture. As the shear rate increases, there is a drastic fall in viscosity, which in turn reduces the elastic strain energy of the molecules in the die, thereby lowering the recovery at the exit.¹¹ As seen from the results of studies at lower shear rates (discussed later), the critical shear rate, defined as the shear rate at and beyond which melt fracture occurs, is well below the shear rates used here. Therefore, a part

of the stored energy is released by the surface tearing of the extrudates that in turn results in decreased die swell. The difference in die swell with increasing shear rate diminishes with increasing W-EPDM loading when the melt fracture becomes less prominent. This can also be due to the increasing rubber–filler interaction, which in turn hinders the uncoiling and recoiling of polymer chains and giving negligible changes in the extrudate swell.

An increase in die swell is observed with an increase of temperature, which is believed to be attributable to the onset of crosslinking of the matrix rubber (R-

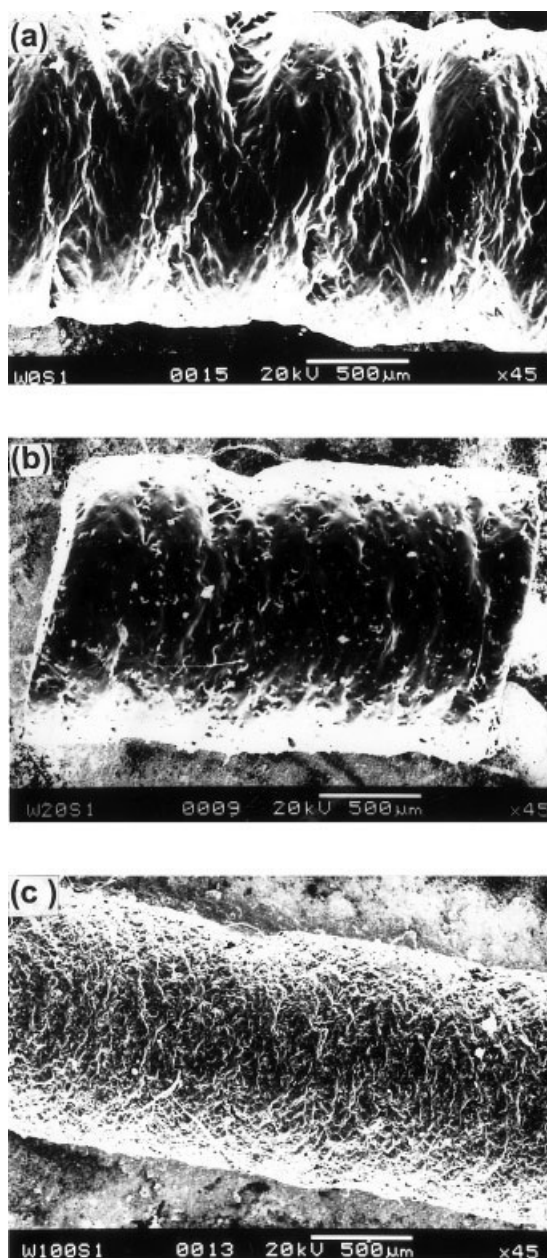


Figure 7 Representative SEM photomicrographs of the extrudates at 110°C and at 306.7 s⁻¹: (a) W₀, (b) W₂₀, and (c) W₁₀₀.

EPDM) increasing the compound elasticity. While moving through the capillary, the polymer chains uncoil and extend or orient; at the die exit they recoil more because of the already formed crosslinks. The increase of die swell with temperature diminishes as the W-EPDM content increases (Fig. 8). As loading of W-EPDM increases, the R-EPDM proportion decreases. Consequently, the polymer chains that are free to uncoil and recoil, which contributes to the die swell, become less available. Therefore, the effect of temperature is negligible at higher loadings of W-EPDM.

Rheological behavior of compounds in low shear rate region

Because the R-EPDM compound shows a high degree of distortion in the range of apparent shear rates used ($306.7\text{--}1533.2\text{ s}^{-1}$), it is evident that the $\dot{\gamma}_{\text{crit}}$ of the compound lies below 306.7 s^{-1} . In order to study the variation of the $\dot{\gamma}_{\text{crit}}$ with W-EPDM loading, processability studies were made in the low shear rate region ($<306.7\text{ s}^{-1}$).

Typical log-log plots of the apparent viscosity and apparent shear stress at 110°C are given in Figure 10. Up to an apparent shear rate of 61.3 s^{-1} , the viscosity of the compounds increases with the W-EPDM loading. A similar observation was made in the case of the

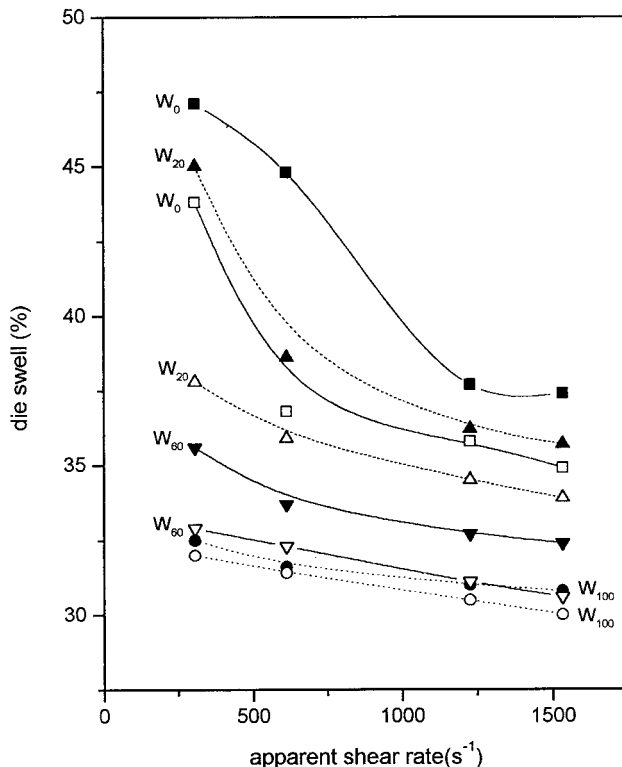


Figure 8 The running die swell (%) as a function of the W-EPDM content, apparent shear rate, and temperature at (filled symbols) 110° and (open symbols) 90°C .

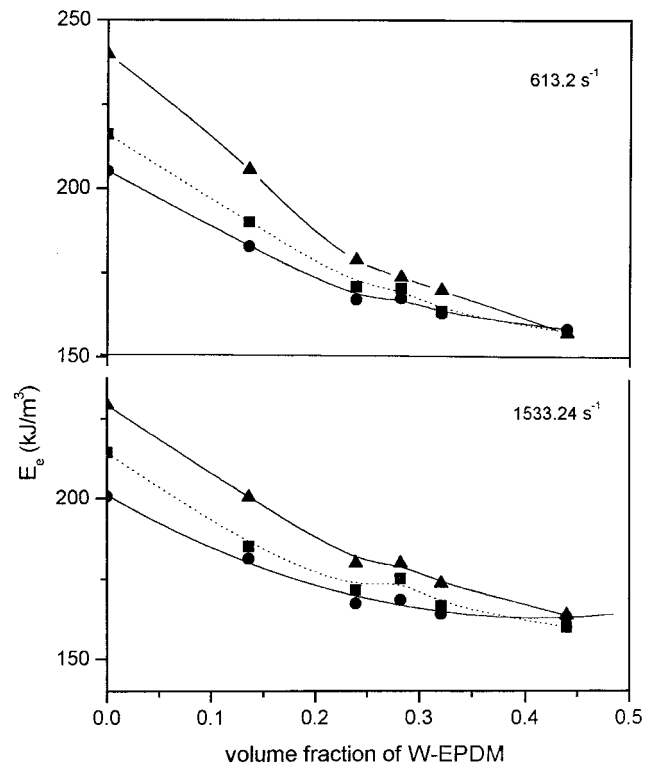


Figure 9 Representative plots showing the variation of the stored elastic energy (E_e) with W-EPDM loading, shear rate, and temperature at (●) 90° , (■) 100° , and (▲) 110°C .

Mooney viscosity measurements.¹⁸ The onset of wall slip is evident in the lowering of the viscosity beyond 61.3 s^{-1} . As the shear rate increases, slip dominates and the apparent viscosity of W_{50} and W_{100} decreases. In general, the onset of slip occurs at lower shear rates with the increase of W-EPDM loading and the increase of the temperature, because the amount of oil increases with increasing W-EPDM content. This is in agreement with the inversion of viscosity observed at shear rates in the region of $300\text{--}1533\text{ s}^{-1}$, as discussed earlier in this article.

It is known that as the shear rate increases, the extrudate distortion begins at a particular shear rate that is termed the critical shear rate and it depends upon the nature of the rubber compound.²² The representative SEM photomicrographs of typical extrudates at and around the critical shear rate are shown in Figure 11. As the loading of W-EPDM in the compound increases, the critical shear rate increases (Table V). This effect is similar to that observed in carbon black filled rubber compounds where carbon black broadens the shear rate range in which smooth extrudates are obtained.^{11,34} For highly loaded compounds the severity of melt fracture is very low at all shear rates and temperatures.

Representative plots of the die swell against the apparent shear rate at different temperatures are shown in Figure 12. The compounds show maximum

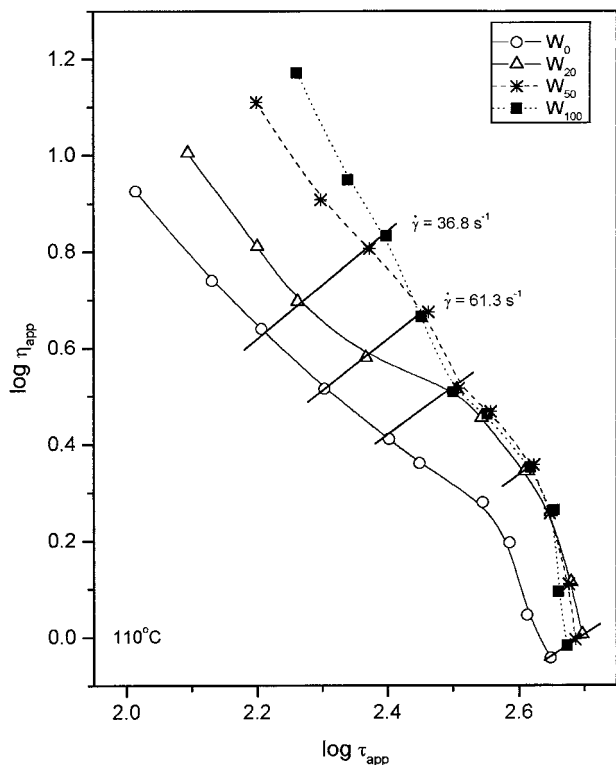


Figure 10 Typical log-log plots of the apparent viscosity (η_{app}) and shear stress (τ_{app}) at 110°C in the low shear rate region (η_{app} in kPas and τ_{app} in kPa).

TABLE V
Critical Shear Rate ($\dot{\gamma}_{crit}$) for Representative Compounds at Different Temperatures

Mix No.	$\dot{\gamma}_{crit}$ (s ⁻¹)		
	90°C	100°C	110°C
W_0	61.3	98.1	122.6
W_{20}	61.3	122.6	122.6
W_{50}	98.1	184.0	184.0
W_{100}	184.0	184.0	368.0

die swell just before the critical shear rate. The maximum die swell increases with the temperature. It can be seen that the particular shear rate up to which the die swell of the compounds increases with the shear rate ($\dot{\gamma}_{max}$) is a characteristic of the compound and dependent on the temperature. As the W-EPDM content in the compound increases, the $\dot{\gamma}_{max}$ shifts to a higher value; and in the highly filled compounds (W_{50} , W_{100}) the effect is negligible at all temperatures, and the die swell remains more or less constant in a broader range of shear rates.

Effect of carbon black, oil, and crosslinked rubber particles on die swell and extrudate distortion

The die swell values of W_0 (unfilled), W_{20} , W_{20B} , W_{20G} , and W_{20L} are plotted versus the apparent shear rate in

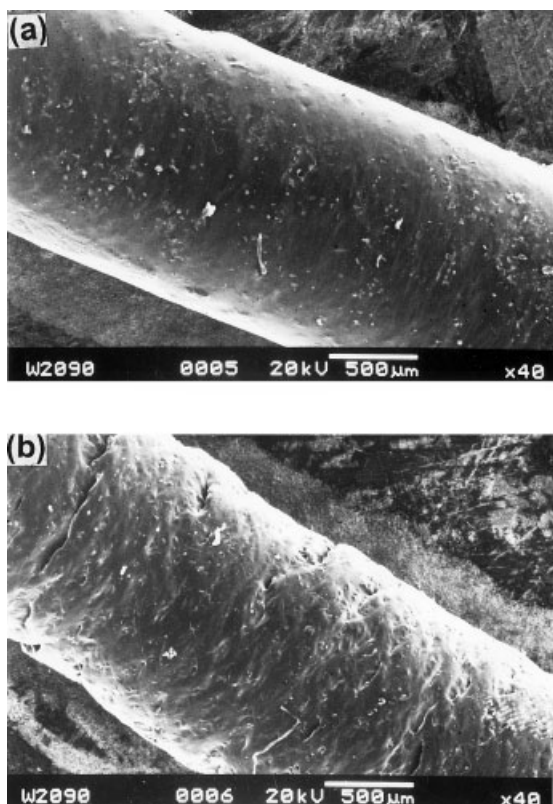


Figure 11 Typical SEM photomicrographs of the extrudates at and around the critical shear rate at 90°C for W_{20} at (a) 24.5 and (b) 61.3 s⁻¹.

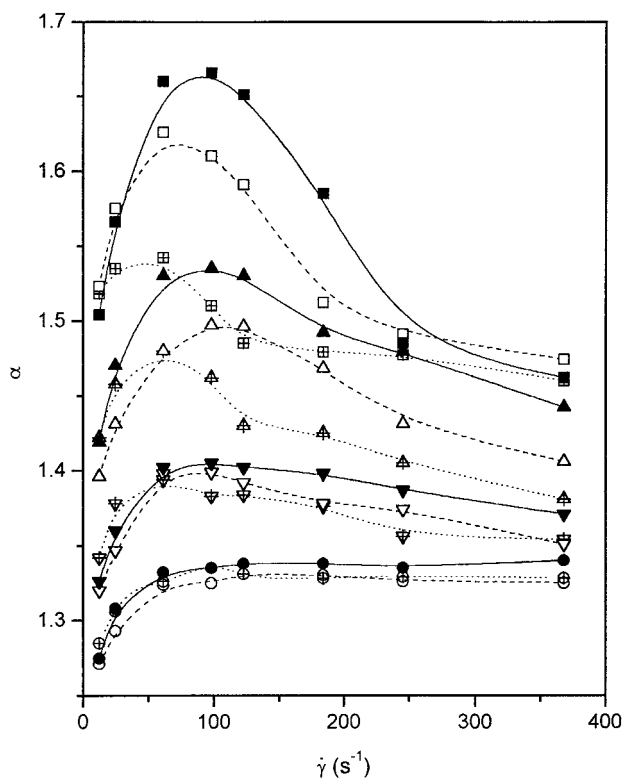


Figure 12 Representative plots of the die swell versus the shear rate at different temperatures in the low shear rate region ($\boxplus, \square, \blacksquare$) W_0 , ($\Delta, \blacktriangle, \triangle$) W_{20} , ($\nabla, \blacktriangledown, \triangledown$) W_{50} , and (\oplus, \circ, \bullet) W_{100} . \cdots 90°C, $---$ 100°C, $—$ 110°C

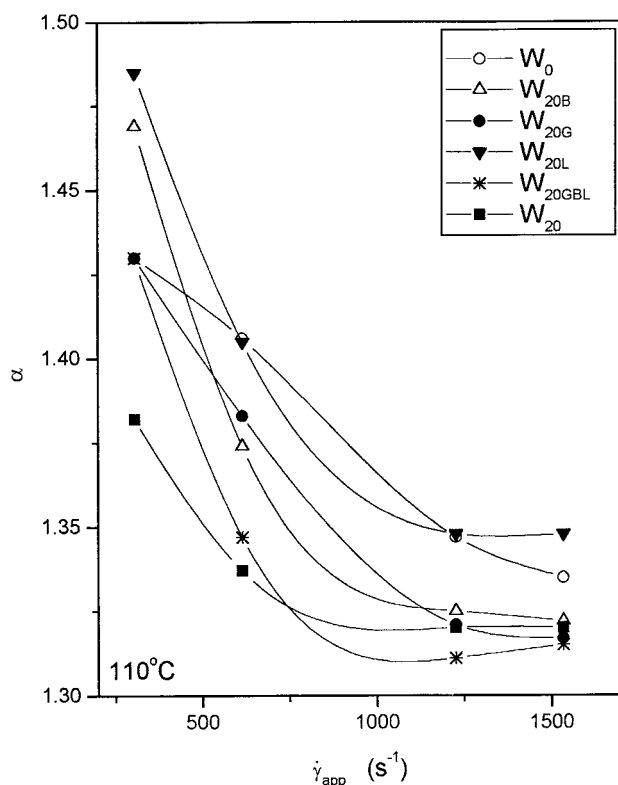


Figure 13 Plots of the die swell versus the apparent shear rate for the control compounds at 110°C.

Figure 13. The last three compositions contain the same proportions of carbon black, W-EPDM(G), and oil as in W_{20} . Formulation W_{20GBL} contains carbon black, oil, and crosslinked polymer together, as in W_{20} .

The presence of black or crosslinked gum powder is found to reduce the die swell in the shear rate range that we used, but the effectiveness of the gum powder in cutting down the elastic energy (W_{20G}) and thereby the die swell is higher than the carbon black (W_{20B}) present in the W-EPDM. Adding oil is found to increase the die swell when the values are compared at a constant shear rate. The presence of the three components together as in W_{20GBL} drastically reduces the die swell at all shear rates, as is also observed in the case of W_{20} . The effect of oil is overshadowed by the presence of carbon black and gum powder in W_{20GBL} .

It can be seen that the extrudate distortion is reduced to a greater extent by the W-EPDM(G) than by the black or oil (Fig. 14). Thus, the reduction in distortion by the addition of W-EPDM is mainly contributed by the crosslinked polymer in W-EPDM. However, because the $\dot{\gamma}_{crit}$ for all these compounds is below the shear rate range used, all compositions show distortion.

CONCLUSIONS

1. The shear viscosity of the EPDM compounds at high shear rates is decreased by the addition of

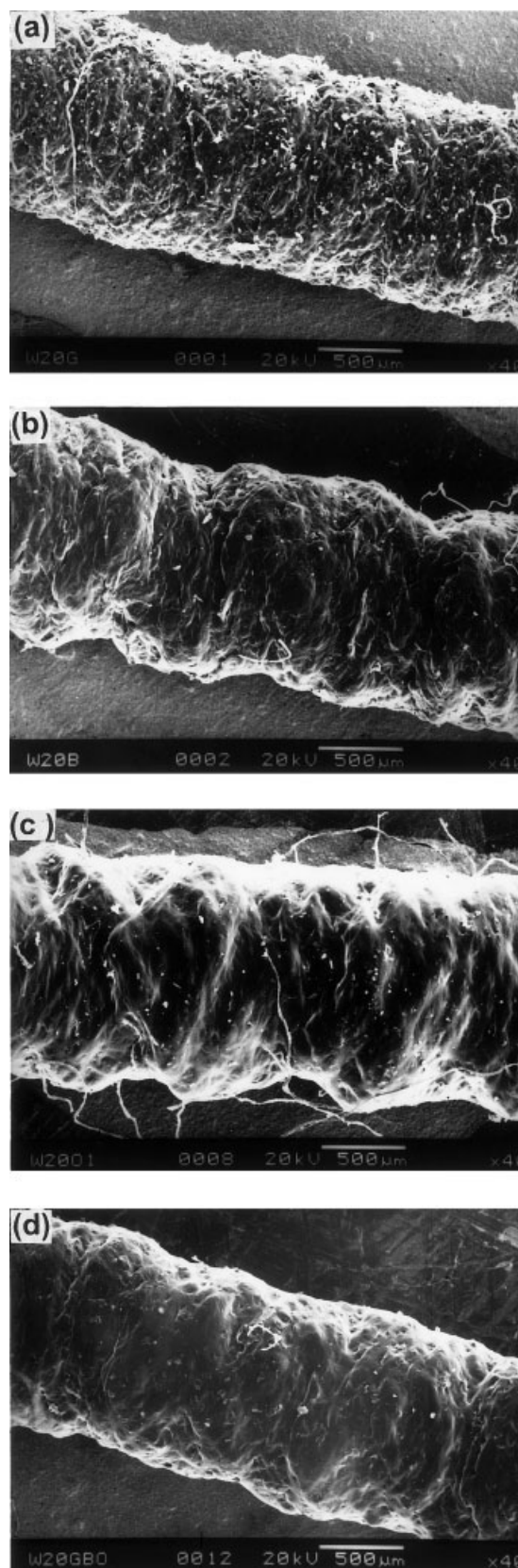


Figure 14 SEM photomicrographs of the extrudates of control compounds at 110°C: (a) W_{20G} , (b) W_{20B} , (c) W_{20L} , and (d) W_{20GBL} .

ground EPDM vulcanizate (W-EPDM), presumably because of plasticizer migration.

2. The die swell of the extrudate is decreased by the addition of W-EPDM, which is primarily due to the synergistic effect of carbon black and crosslinked polymer present in W-EPDM.
3. With increasing shear rate the die swell decreases whereas with increasing temperature the die swell increases slightly. This is presumably attributable to the opposing effects of a reduction in viscosity with shear rate and a slight increase of elasticity due to the onset of vulcanization at higher temperatures.
4. The addition of W-EPDM reduces the extent of extrudate distortion, which may be due to the increased viscosity of the compound outside the die.
5. As the amount of W-EPDM in the compound increases, the critical shear rate increases. In other words, the extrudate surface remains undistorted over a wider shear rate range.
6. Utilization of W-EPDM in R-EPDM provides processing advantages like decreased die swell and less extrudate distortion.

The authors gratefully acknowledge the financial assistance and sponsorship by the Ministry of Environment and Forests, Government of India, New Delhi. Thanks are also due to Mr. S. Mushtaq for his assistance in carrying out the rheological experiments.

References

1. De, S. K. *Prog Plast Rubber Technol* 2001, 17, 113.
2. Mahlke, D. *Kautsch Gummi Kunst* 1993, 46, 889.
3. Phadke, A. A.; Chakraborty, S. K.; De, S. K. *Rubber Chem Technol* 1984, 57, 19.
4. Dierkes, I. W. *Rubber World* 1996, vol. 214, May, 25.
5. Kim, J. K.; Burford, R. P. *Rubber Chem Technol* 1998, 71, 1028.
6. Phadke, A. A.; Bhowmick, A. K.; De, S. K. *J Appl Polym Sci* 1986, 32, 4063.
7. Norman, R. H.; Johnson, P. S. *Rubber Chem Technol* 1981, 54, 493.
8. Ertong, S.; Eggers, H.; Schummer, P. *Rubber Chem Technol* 1994, 67, 207.
9. Phadke, A. A. *Plast Rubber Proc Appl* 1986, 6, 273.
10. Gibala, D.; Laohapisitpanich, K.; Thomas, D.; Hamed, G. R. *Rubber Chem Technol* 1996, 69, 115.
11. Leblanc, J. L. *Rubber Chem Technol* 1981, 54, 905.
12. Rosen, S. L.; Rodriguez, F. *J Appl Polym Sci* 1965, 9, 1601.
13. Murty, V. M.; Gupta, B. R.; De, S. K. *Plast Rubber Proc Appl* 1985, 5, 307.
14. Osnaiye, G. J.; Arkadii, I. L.; White, J. L. *Rubber Chem Technol* 1995, 68, 51.
15. Markovic, M. G.; Choudhury, N. R.; Dimopoulos, M.; Matison, J. G.; Dutta, N. K.; Bhattacharya, A. K. *Polym Eng Sci* 2000, 40, 1065.
16. Guriya, K. C.; Bhattacharya, A. K.; Tripathy, D. K. *Polymer* 1998, 39, 109.
17. Bhaumik, T. K.; De, P. P.; Gupta, B. R. *Kautsch Gummi Kunst* 1989, 42, 115.
18. Jacob, C.; De, P. P.; Bhowmick, A. K.; De, S. K. *J Appl Polym Sci* 2001, 82, 3293.
19. Jacob, C.; De, P. P.; Bhowmick, A. K.; De, S. K. *J Appl Polym Sci* 2001, 82, 3304.
20. Padovan, J.; Prasad, N.; Gerrard, D.; Park, S. W.; Lindsley, N. *Rubber Chem Technol* 1999, 72, 343.
21. *Operation and Service Manual—Monsanto Processability Tester*; Monsanto Co., St. Louis, MO.
22. Brydson, J. A. *Flow Properties of Polymer Melts*, 2nd ed.; George Godwin Ltd: London, 1981; Chapter 1.
23. Vinogradav, G. V.; Malkin, A. Ya. *Rheology of Polymer Melts*; Mir Publishers: Moscow, 1980.
24. Kumar, N. R.; Bhowmick, A. K.; Gupta, B. R. *Kautsch Gummi Kunst* 1992, 45, 531.
25. Roy, D.; Bhattacharya, A. K.; Gupta, B. R. *J Elast Plast* 1993, 25, 46.
26. Phadke, A. A.; Kuriakose, B. *Kautsch Gummi Kunst* 1985, 38, 694.
27. Turner, D. M.; Moore, M. D. *Plast Rubber Proc Appl* 1980, 1, 81.
28. Turner, D. M.; Bickley, A. C. *Plast Rubber Proc Appl* 1981, 1, 357.
29. Fujimoto, K.; Nishi, T.; Okamoto, T. *Int Polym Sci Technol* 1980, 8(8), 30.
30. Sharapova, I. N.; Chekanova, A. A.; Zakharov, N. D.; Borisova, E. Yu. *Int Polym Sci Technol* 1983, 10(2), 5.
31. Fujimoto, K.; Nishi, T. *Int Polym Sci Technol* 1981, 8(11), 25.
32. Isayev, A. I.; Wan, M. *Rubber Chem Technol* 1996, 69, 277.
33. Rosen, S. L.; Rodriguez, E. L. *J Appl Polym Sci* 1965, 6, 1615.
34. Hopper, J. R. *Rubber Chem Technol* 1967, 40, 463.